

# Accelerated Particles from Shocks Formed in Merging Clusters of Galaxies

Robert C. Berrington , Charles D. Dermer<sup>†</sup> and S. J. Sturmer

*ASEE Postdoctoral Fellow, Naval Research Laboratory, Code 7653, Washington, DC 20375-5352*

*<sup>†</sup>Naval Research Laboratory, Code 7653, Washington, DC 20375-5352*

*NASA's GSFC and USRA, 7501 Forbes Blvd. #206, Seabrook, MD 20706-2253*

**Abstract.** Subcluster interactions within clusters of galaxies produce shocks that accelerate non-thermal particles. We treat Fermi acceleration of nonthermal electrons and protons by injecting power-law distributions of particles during the merger event, subject to constraints on maximum particle energies. The broadband nonthermal spectrum emitted by accelerated electrons and protons is calculated during and following the subcluster interaction for a standard parameter set. The intensity of  $\gamma$ -ray emission from primary and secondary processes is calculated and discussed in light of detection capabilities at radio and  $\gamma$ -ray energies.

## INTRODUCTION

Rich clusters contain thousands of galaxies and are the largest gravitationally bound systems in nature. Masses for rich clusters are  $10^{15}M_{\odot}$ , with 5–10% of the mass found in a hot intergalactic gas at temperatures of 2–12 keV. Rich clusters emit thermal bremsstrahlung with luminosities  $L_x \approx 10^{44} - 10^{45} \text{ ergs s}^{-1}$  [1]. Poor clusters contain hundreds of galaxies, have total masses  $10^{14}M_{\odot}$ , have a hot intergalactic gas of temperatures 1–5 keV and X-ray luminosities  $L_x \approx 10^{42} - 10^{43} \text{ ergs s}^{-1}$  [2]. Approximately 90% of the total mass of clusters is in the form of nonluminous dark matter.

In the hierarchical merging cluster scenario, poor clusters merge together to form richer clusters. Approximately 30–40% of galaxy clusters show evidence of substructure in both the optical [3] and X-ray wavelengths [4]. Velocity differences between the observed structures is  $1000\text{--}2000 \text{ km s}^{-1}$ . With gravitational forces driving the interaction between the two systems, cluster mergers are consistent with highly-parabolic orbits. Typical sound speeds within the intergalactic medium (IGM) are  $800 \text{ km s}^{-1}$ , so shocks will form at the interaction boundary of the two systems. Computer models of merging clusters support the development of shocks in the IGM [5, 6, 7]. Dimensional arguments show that a cluster merger releases  $10^{63} - 10^{64}$  ergs of gravitational potential energy when initial separations are of the order  $1 \text{ Mpc}$ .

Only the most massive and X-ray luminous galaxy clusters have extended diffuse radio sources. With projected linear sizes  $> 1 \text{ Mpc}$ , these diffuse sources have no known optical counterparts. The diffuse radio emissions have two distinct characteristics. The extended diffuse emission found in the central region of a galaxy cluster with a regular, azimuthally symmetric shape is known as a *radio halo*. The diffuse emission found on the cluster periphery are the cluster *radio relics*. These features often have irregular

shapes with signs of filamentary structure. Radio relics are associated only with clusters that show evidence of a recent or ongoing merger event.

Shock fronts that form in the IGM as a result of a cluster merger event are thought to be associated with the cluster radio relics. The shock compression will orient any existing cluster magnetic field into the plane of the shock. Radio relics are characterized by highly organized magnetic fields with field strengths in the  $\sim 1 \mu\text{G}$  range with linearly polarized field lines in the vicinity of the shock [8]. The shock front will accelerate a fraction of the thermal particles within the IGM by first-order Fermi acceleration.

Recent work has highlighted the importance of nonthermal radiation from particles accelerated by shocks formed in merging clusters. Loeb and Waxman [9] have proposed that cluster mergers are the dominant contributor to the diffuse  $\gamma$ -ray background, provided the efficiency to convert the available gravitational energy into nonthermal electron energy is  $\sim 5\%$ . Some unidentified EGRET sources are claimed to be associated with  $\gamma$ -ray emission from galaxy clusters [10]. Excess EUV emission from Coma can be explained by nonthermal electrons accelerated at merger shocks [11]. Variations in radio surface brightness will result from superposition of cluster emissions [12].

In order to examine this question in more detail, we have modified a supernova remnant code [13] to calculate nonthermal radiation spectra from primary and secondary particles in merger shocks. We go beyond previous treatments by considering both primary electron and proton acceleration, a time-dependent treatment of radiation losses, and radiation signatures of secondaries from proton-nuclear interactions.

## MODEL

We have adapted a supernova remnant code [13] to treat the cluster merger scenario. The code is designed to calculate time-dependent particle distribution functions evolving through adiabatic and radiative losses for electrons and protons accelerated by the first-order Fermi process at the cluster merger shock.

The electron and proton distribution functions originate from a momentum power-law injection spectrum. In terms of total particle energy  $E = m\gamma c^2$ , the injection function is

$$Q_{e;p}(E;t) = Q_{e;p}^0 \frac{(pc)^s}{\beta} \exp\left[-\frac{E}{E_{max}(t)}\right]; \quad (1)$$

where  $p = \beta\gamma$  is the dimensionless momentum and  $s$  is the injection index. The maximum particle energy  $E_{max}$  is determined by the maximum energy associated with the available time since the beginning of the merger event, by a comparison of the Larmor radius with the size scale of the system, and by a comparison of the energy-gain rate through first-order Fermi acceleration with the energy-loss rate due to adiabatic, synchrotron and Compton processes. Particle injection ceases after the age of the shock front exceeds  $t_{acc} = 10^9$  yrs. The constant  $Q_{e;p}^0$  normalizes the injected particle spectrum over the entire volume  $V(t)$  swept out by the shock front, and is determined by

$$E_{e;p}^{tot} = \int_0^{t_{acc}} dt \int_0^{E_{max}} dE E Q_{e;p}(E;t) V(t); \quad (2)$$

We assume a total available energy  $E_{e;pp}^{tot} = \eta_{e;pp} 10^{63}$  ergs, and an efficiency factor  $\eta_{e;pp} = 5\%$  for both protons and electrons. Although the injection index  $s$  depends upon the Mach number of the shock, here we present calculations for a fixed index  $s = 2$ .

The time evolving particle spectrum is determined by solving the Fokker-Planck equation in energy space for a spatially homogeneous IGM, given by

$$\frac{\partial n(E;t)}{\partial t} = \frac{\partial}{\partial E} [\dot{E}_{tot}(E;t)n(E;t)] + \frac{1}{2} \frac{\partial^2}{\partial E^2} [D(E;t)n(E;t)] + Q(E;t) - \frac{n(E;t)}{\tau_{pion}(E;t)} : (3)$$

The quantity  $\dot{E}_{tot}(E;t)$  represents the total synchrotron, Compton, Coulomb, and adiabatic energy-loss rate for electrons, and the sum of the Coulomb and adiabatic energy-loss rates for protons. Both protons and electrons are subject to diffusion in energy space by Coulomb interactions. The protons experience catastrophic losses due to proton-proton collisions on the time scale  $\tau_{pion}$ . The spectra of secondary electrons and positrons are calculated from pion-decay products, and are subject to the same physical processes as the primary electrons.

The synchrotron, Compton, bremsstrahlung, and pion-decay  $\gamma$ -ray spectral components are calculated from the particle spectra following the methods described by Sturner, *et al.* [13]. We use a standard parameter set with a mean IGM number density  $n_{IGM} = 10^{-3} \text{ cm}^{-3}$ , a uniform cluster magnetic field of  $B = 0.1 \mu\text{G}$ , a constant shock speed  $v_s = 1000 \text{ km s}^{-1}$ , and an acceleration period of 1 Gyr. Thus,  $V(t) = A(t)v_s t$ . We assume a constant surface area with a 1 Mpc radius. Particles lose energy due to adiabatic expansion according to the relation  $\dot{\gamma} = \dot{V} = V(t) = 1/t$ .

## RESULTS AND DISCUSSION

Figure 1 shows nonthermal photon spectra calculated at 1 Gyr and 5 Gyr for our standard parameters. The system is very luminous at radio frequencies during the particle acceleration phase because of intense Compton losses of nonthermal electrons on the CMB. After the acceleration period ends, the radiation from primary electrons is dominated by emission from secondaries. The  $\pi^0$  bump at 70 MeV is hidden beneath the Compton-scattered CMB radiation from primary electrons during the acceleration period, but dominates the  $\gamma$ -ray spectrum after the acceleration period is over. The intensity of the  $\pi^0$  bump depends sensitively upon the relative efficiencies  $\eta_{p,e}$  for proton and electron acceleration. If no pion signature is found in nonthermal  $\gamma$  rays from merging clusters, then  $\eta_p < \eta_e$  for our standard parameters.

From the total photon spectra in Figure 1, we have calculated light curves at various photon energies in Figure 2 for a merging cluster at a distance of 100 Mpc. The maximum peak 1.4 GHz radio flux density of  $\sim 12 \text{ Jy}$  occurs at the end of the acceleration period. The radio emission from the merger event is, however, distributed over an angular region  $\sim 0.5$  of the merger shock, making it difficult to detect.

Figure 2 presents calculations of the energy fluxes from a merger shock at 100 Mpc, for photon energies  $> 100 \text{ MeV}$ ,  $> 1 \text{ GeV}$ , and  $> 300 \text{ GeV}$ . The maximum luminosity occurs at the end of the acceleration period due to the accumulation of nonthermal protons. Cooling times due to synchrotron and Compton energy losses are very short for

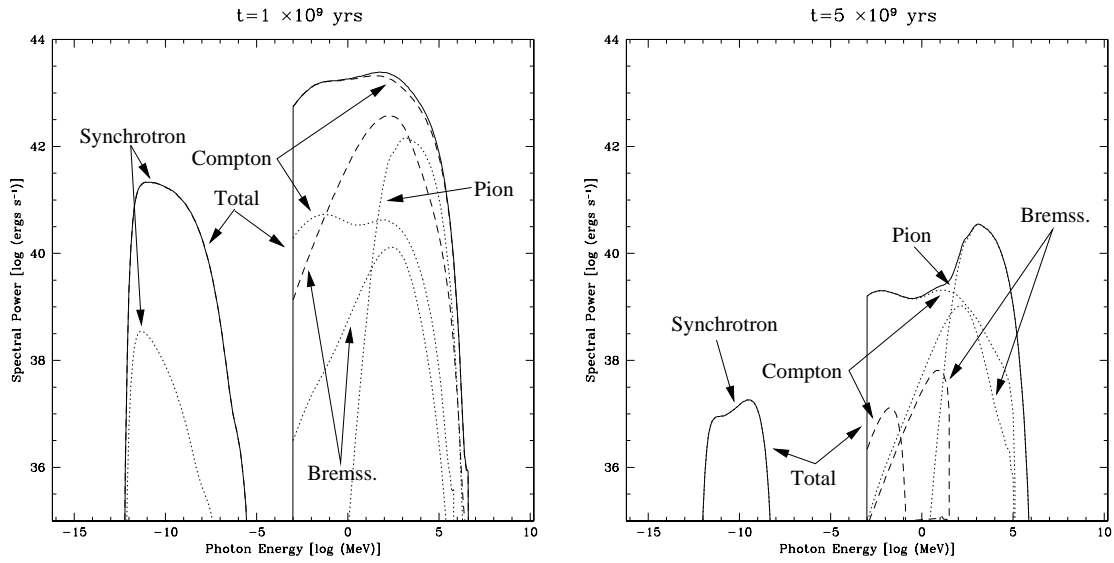


**FIGURE 1.** Total nonthermal photon energy spectra from a cluster merger shock. The solid curves are the total photon spectra summed from all processes. The dashed curves are the photons produced from the primary electrons, and the dotted curves are the secondary emission components. The left and right panels show the total nonthermal photon spectra at  $t = 1$  Gyr and  $t = 5$  Gyr, respectively, after the onset of the cluster merger event.

high-energy electrons; electrons that Compton-scatter microwave photons to energies  $E = 100E_{100}$  MeV will cool on a time scale of  $t_{cool} = 6 \times 10^6 \frac{E}{E_{100}}$  yrs. Consequently, the  $\gamma$ -ray emission declines sharply after particle acceleration ceases, and approaches a level where all the  $\gamma$ -ray production originates from proton interactions. The maximum flux for secondary electrons is 2 orders of magnitude less than the maximum flux for the primary electrons, as can be seen by comparing the catastrophic proton loss time scale of 30 Gyr with the 1 Gyr injection time scale. Because of adiabatic losses and the long catastrophic pion production cooling times, protons inject a slowly declining rate of secondary electrons in the 1-4 Gyrs after the initial acceleration event.

## SUMMARY

We have studied the acceleration of protons and electrons in shocks formed by merging clusters of galaxies, and calculated the expected synchrotron, Compton, bremsstrahlung, and pion emission from the accelerated particles. Both the radio flux density at 1.4 GHz and the  $\gamma$ -ray flux at photon energies  $> 100$  MeV,  $> 1$  GeV and  $> 300$  GeV for a source at 100 Mpc as a function of time are presented. The flux is greatest at the end of the particle acceleration phase, and merging clusters of galaxies at a characteristic distance of 100 Mpc should be detectable with radio telescopes and GLAST. Radio and  $\gamma$ -ray detectability of merger events must contend with the angular extent of the emission.

Because the merger event lasts for only 1 Gyr, a large fraction of clusters will no longer be experiencing ongoing nonthermal particle acceleration from cluster mergers.

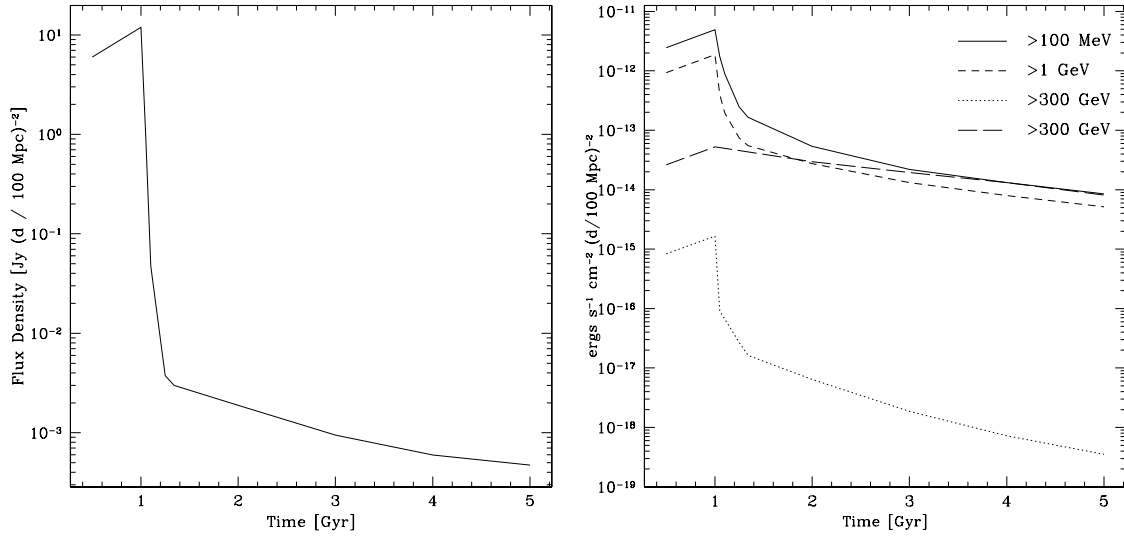


**FIGURE 2.** Calculated 1.4 GHz radio flux density (left panel) and integrated flux of high energy photons (right panel) from a cluster merger shock. Both panels are normalized for a system at a distance of 100 Mpc. The radio flux density is in the 1.4 GHz band, and the integrated energy fluxes for the high energy photons are shown in the right panel. Also shown is the  $> 300$  GeV emission for a merger where  $v_s = 2000 \text{ km s}^{-1}$  and  $B = 1 \mu\text{G}$  as the boldfaced, long-dashed line.

GLAST, with a limiting sensitivity of  $4 \times 10^{13} \text{ ergs cm}^{-2} \text{ s}^{-1}$  for a one year all-sky survey, will still be able to detect such systems if they are at optimal distances. Depending on the shock speed and magnetic field, cluster merger events can also be detectable sources of TeV radiation (see Fig. 2). We therefore expect detectable  $\gamma$ -ray emission from clusters at distances  $\sim 100$  Mpc. Within this distance a number of radio relics have been detected [14, 15].

## REFERENCES

1. Allen, S. W. and Fabian, A. C., *MNRAS*, **269**, 409 (1994).
2. Dahlem, M. and Thiering, I., *Publ. Astr. Soc. Pacif.*, **112**, 148 (2000).
3. Beers, T. C., Geller, M. J., & Huchra, J. P., *ApJ*, **257**, 23 (1982).
4. Forman, W., *et al.*, *ApJ*, **243**, L133 (1981).
5. Roettiger, K., Burns, J., and Loken, C., *ApJL*, **407**, 53 (1993).
6. Ricker, P. M., *ApJ*, **496**, 670 (1998).
7. Takizawa, M., *ApJ*, **520**, 514 (1999); *ApJ*, **532**, 183 (2000).
8. EnBlin, T. A., *et al.*, *Astron. & Astrophys.*, **332**, 395.
9. Loeb, A. and Waxman, E., *Nature*, **405**, 156 (2000).
10. Colafrancesco, S. and Blasi, P., *Astroparticle Physics*, **9**, 227 (1998).
11. Atoyan, A. M. and Völk, H. J., *ApJ*, **535**, 45 (2000).
12. Waxman, E. and Loeb, A., *ApJ*, **545**, L11 (2000).
13. Sturmer, S. J., *et al.*, *ApJ*, **490**, 619 (1997).
14. Giovammini, G. and Feretti, L., *New Astronomy*, **5**, 335 (2000).
15. Kempner, J. C. and Sarazin, C. L., *ApJ*, **548**, 639 (2001).